Available online at www.sciencedirect.com

SCIENCE DIRECT®

Thin Solid Films 492 (2005) 195 – 202

thin solid films

www.elsevier.com/locate/tsf

Measurement of residual stress and elastic modulus of polycrystalline 3C-SiC films deposited by low-pressure chemical vapor deposition

Xiao-an Fu *, Jeremy L. Dunning, Christian A. Zorman, Mehran Mehregany

Department of Electrical Engineering and Computer Science, Case Western Reserve University, Cleveland, OH 44106, USA

Received 23 November 2004; received in revised form 20 June 2005; accepted 11 July 2005
Available online 16 August 2005

Abstract

Residual stress and in-plane biaxial modulus of polycrystalline 3C-silicon carbide (poly-SiC) films are studied using bulk and surface micromachined microstructures. The poly-SiC films are deposited on 100-mm-diameter (100) silicon wafers in a high-throughput, low-pressure chemical vapor deposition furnace at 1173 K using dichlorosilane (SiH_2Cl_2) and acetylene (C_2H_2) precursors at deposition pressures from 61 to 666 Pa. The resulting 0.5 to 2.7 μm films are highly textured, (111) oriented, polycrystalline 3C-SiC. Suspended diaphragms of these films are fabricated by standard wet chemical bulk micromachining of the silicon substrate from the back side. The load-deflection technique is used to extract the residual stress and in-plane biaxial modulus. For the center slot position in the boat, the films' residual stress changes from high (e.g., 726 MPa) to a relatively lower (e.g., 265 MPa) tensile stress as the deposition pressure increases from 61 to 333 Pa at fixed precursor flow rates. The average biaxial modulus of the films is 482 GPa; accordingly, the average Young's modulus is 401 GPa, assuming a Poisson's ratio of 0.168. However, the poly-SiC diaphragms fabricated from films deposited in the 380 to 666 Pa pressure range buckle due to compressive residual stress. Therefore, micro strain gauges are also fabricated and used to measure compressive residual strains in these films, which are −0.032% at 500 Pa and −0.024% at 666 Pa. Using 401 GPa as Young's modulus, these correspond to residual stresses of −129 MPa and −98 MPa, respectively.
© 2005 Elsevier B.V. All rights reserved.

Keywords: Silicon carbide; Chemical vapor deposition (CVD); Elastic properties; Stress

1. Introduction

Semiconductor-grade SiC is an attractive material for microelectromechanical systems (MEMS) because of its outstanding mechanical, chemical, and electrical properties [1,2], which enable the development of solid-state transducers for applications in harsh environments [3–5]. For example, sensor applications that require operational capability in high temperature, high radiation, corrosive, and/or erosive environments are beyond the reach of silicon technology but are enabled by SiC due to its unique material properties. In order to advance SiC semiconductor technology to support such applications, the development of material deposition and fabrication process technologies, including material and process characterization, is critical and much progress has already been made [1–9]. For example, in addition to bulk micromachining [10–12], surface micromachining processes that generally parallel the capabilities of those of polysilicon (poly-Si) based processes, but are based on polycrystalline 3C-SiC (poly-SiC), have been demonstrated [5,6,13] and poly-SiC MEMS devices have been successfully operated at 823 K [14,15] and beyond [16].

Current emphasis regarding the poly-SiC technology is to reduce the deposition temperature and increase wafer throughput and size, paralleling poly-Si capabilities [5–9]. To this end, low-pressure chemical vapor deposition processes (LPCVD) in hot-wall tube furnaces are being utilized that allow practical (i.e., considering deposition rate and film quality) deposition temperatures around 1073 to 1173 K [5–9]. Accordingly, this paper reports the results of our work in characterizing the residual stress and elastic modulus of LPCVD poly-SiC films deposited at 1173 K

* Corresponding author. Tel.: +1 216 368 4593; fax: +1 216 368 6039.
E-mail address: xxf@cwru.edu (X. Fu).

0040-6090/$ - see front matter © 2005 Elsevier B.V. All rights reserved.
doi:10.1016/j.tsf.2005.07.236

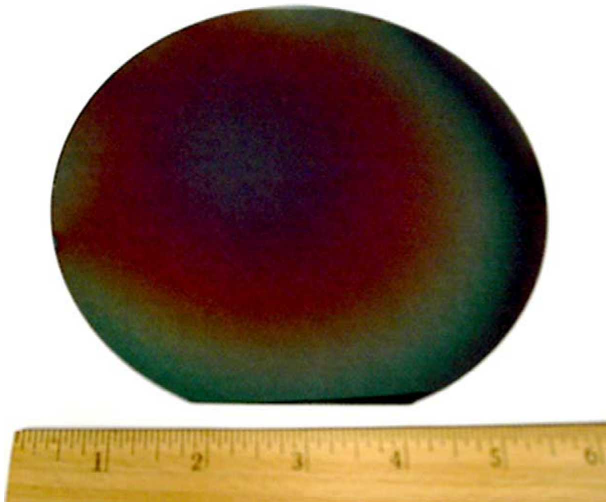

Fig. 1. Optical photo of a 0.75-μm-thick poly-SiC film deposited on a 150-mm-diameter (100) silicon wafer at 1173 K by LPCVD using SiH_2Cl_2 and C_2H_2 precursor gases.

using SiH_2Cl_2 and C_2H_2 at deposition pressures from 61 to 666 Pa. Residual stress and elastic modulus are two of the most important material mechanical properties in the design of MEMS devices.

2. Background

The residual stress and elastic modulus of thin films can vary significantly under different deposition conditions. The load-deflection method has been proven as an effective method for determining residual stress and in-plane biaxial modulus of thin films [17–19]. It has been used to determine elastic modulus and residual stress of 3C-SiC deposited by atmospheric pressure chemical vapor deposition (APCVD) [20–23] and poly-SiC films deposited by LPCVD [24–26]. The published values for the Young's modulus of poly-SiC lie within the range of 350 to 510 GPa [23–26]. Most recently, a Young's modulus for poly-SiC deposited by LPCVD was estimated to be 710 GPa from microfabricated resonator testing [27]. Crystalline microstructure is an important factor in determining the film's residual stress [8] and Young's modulus [23]. For example, Young's modulus of poly-SiC films deposited by APCVD at 1553 K on as-deposited poly-Si was ~350 GPa, while the corresponding value of poly-SiC films deposited on poly-Si after annealing prior to poly-SiC deposition was around 460 GPa [23].

In this work, load-deflection measurements on bulk micromachined diaphragms were used to determine the in-plane biaxial modulus and residual tensile stress of poly-SiC films deposited by LPCVD at pressures from 61 to 333 Pa. Poly-SiC films deposited at pressures from 380 to 666 Pa exhibited compressive stress and the microfabricated diaphragms buckled, which rendered the use of the load-deflection method ineffective. Therefore, micro strain gauges were additionally fabricated and used to measure compressive residual strain of the films. Micro strain gauges have the advantage of identifying tensile and compressive residual stresses immediately after fabrication and release by inspection of the devices under an optical microscope [28].

3. Experimental details

Poly-SiC thin films were deposited on 100-mm-diameter (100) silicon wafers in a large-volume, LPCVD furnace using SiH_2Cl_2 and C_2H_2 precursors as described elsewhere [8,9]. It is noteworthy that high quality films with good uniformity (e.g., 7%) have been deposited on 150-mm-diameter silicon wafers (Fig. 1) in this reactor and generally correlate well with the films deposited on the 100-mm-diameter Si wafers under similar conditions.

For the first set of samples (see Tables 1 and 2), pressure was varied from 61 to 666 Pa, while temperature was 1173 K; SiH_2Cl_2 and C_2H_2 (5% in H_2) flow rates were 54 sccm and 180 sccm, respectively. SiH_2Cl_2 and C_2H_2 were injected along the boat from underneath the wafers through two quartz injection tubes. In these depositions, one wafer was placed in each slot in the boat, resulting in poly-SiC deposition on both sides of the wafers. Film thicknesses were in the range of 0.46 to 0.65 μm for the wafers studied from these runs. For the second set of samples (see Table 3), pressure and temperature were kept constant at 267 Pa and 1173 K, SiH_2Cl_2 flow rate was reduced to 35 sccm, C_2H_2 flow rate was 180 sccm, and deposition time was 573 min. In the second deposition set, the precursors entered the reactor from the load end of the furnace without the use of injection tubes. Two wafers were placed back-to-back in each slot of the boat, resulting in poly-SiC deposition only on the front side of the wafers (this scheme simplified backside patterning of diaphragm etch windows by avoiding

Table 1
Average residual stress, biaxial modulus, and Young's modulus (i.e., for $v=0.168$) values for poly-SiC films from three different deposition pressures and fixed deposition temperature of 1173 K, SiH_2Cl_2 flow rate of 54 sccm, and C_2H_2 flow rate of 180 sccm

Deposition pressure (Pa)	Boat slot	Dep. time (min)	Thickness (μm)	σ_o (MPa)	$E/(1-v)$ (GPa)	E (GPa)
61	13	210	0.65	726	519	432
133	13	120	0.46	584	451	375
333	13	120	0.52	265	458	381
					Ave. 476	396

(Boat slot 13 is the center slot of the 25-wafer boat.)

Table 2
Average residual strain and stress (i.e., assuming a Young's modulus of 401 GPa) measured by micro strain gauges for poly-SiC films from three different deposition pressures and fixed deposition temperature of 1173 K, SiH_2Cl_2 flow of 54 sccm, and C_2H_2 flow of 180 sccm

Deposition pressure (Pa)	Boat slot	Dep. time (min)	Thickness (μm)	Strain (%)	σ_o (MPa)
333	20	120	0.52	0.041	165
500	20	96	0.49	−0.032	−129
666	20	120	0.61	−0.024	−98

(Boat slot 20 is near the source end of the 25-wafer boat).

the need to etch a thick poly-SiC film). Film thicknesses were in the range of 2.65 to 2.7 μm for the wafers deposited in this run. All films were highly textured, (111) oriented polycrystalline 3C-SiC as determined by X-ray diffraction measurements (XRD) [8]. X-ray photoelectron spectroscopy analysis indicated that the films were all stoichiometric SiC with approximately 1% oxygen incorporation [9].

Suspended poly-SiC diaphragms were fabricated as shown in Fig. 2 using a bulk micromachining process [20–22]. In this work, 1×1 mm^2 poly-SiC diaphragms were created by anisotropic etching of the (100) silicon substrate from the backside using a KOH solution at 328 K. Since poly-SiC is not etched by KOH at the silicon etching temperatures, there was no need to protect the front side poly-SiC films during the anisotropic etching, and the back side poly-SiC was used as etch mask, patterned by reactive ion etching. For the second set of samples described above when poly-SiC films were deposited only on the front side of the silicon wafers, the KOH etch mask on the back sides of the wafers was a 2-μm-thick conventional low-temperature silicon dioxide film deposited by LPCVD. The shape and area of the fabricated poly-SiC diaphragms were kept constant but the thickness of the deposited films varied from 0.46 to 2.70 μm depending on the deposition condition and time as described above. The in-plane biaxial modulus and residual stress were extracted from these micromachined poly-SiC suspended diaphragms using the load-deflection technique, as described in the next section.

Deflection of the suspended diaphragms was measured using an optical interferometry system described previously [22] and highlighted in Fig. 3. Visible light at the wavelength of 540 (±10) nm passed through the interferometer, which was attached to the microscope as shown in Fig. 3. In conducting the measurement, a pressure was initially applied and then reduced gradually, as a result of which the diaphragm center deflection decreased and individual interference rings disappeared. For every ring that disappeared, representing 270 (±5) nm of deflection, a pressure reading was recorded.

The mounting procedure described by Mitchell et al. [22] was followed to ensure no deflection of the substrates during testing. The samples were mounted onto a cylindrical aluminum chuck using Stronghold™ 7036 Blanchard Wax with the diaphragm cavity side up, as shown in Fig. 3, in order to achieve better accuracy in measurement of the in-plane biaxial modulus [22]. The cylindrical chuck, which sat atop the microscope stage, was directly connected to the pressure manifold via a 1-mm-diameter hole in the chuck.

The uncertainties of residual stress and modulus measured by this load-deflection apparatus were studied by Mitchell et al. [22]. The instrumental uncertainties resulted from the measurement of the applied pressure (±0.5%) and deflection (±1.9%). Measurement uncertainty was induced from user error in the measured pressures and displacements. In conducting load-deflection tests, at least three "reliable" measurements (see next section) were made on each sample and more than 10 samples were extracted from each wafer in order to achieve a reasonable statistical analysis. The diaphragm geometry measurement uncertainty resulted from the uncertainty of the measured diaphragm thickness and size (i.e., in-plane length/width). The observed in-plane length/width measurement uncertainty was around 2 μm for 1×1 mm^2 diaphragms. The diaphragm thickness uncertainty was less than ±5% since the deposited poly-SiC film thicknesses were measured by a NanospecAFT 4000 Visible calibrated against SEM cross-sectional measurements on poly-SiC films. The combined uncertainty for residual stress is therefore about 8.5%, while that for Young's modulus is about 9% [22].

Microfabricated micro strain gauges were used to determine the residual stress of the films deposited at 500 and 666 Pa. These films had compressive residual stresses which resulted in buckled diaphragms. The films deposited at 333 Pa, even though under tensile residual stress, were

Table 3
Average residual stress, biaxial modulus, and Young's modulus (i.e., for $\nu=0.168$) values for poly-SiC films from three wafers along the 25-wafer boat in the same deposition run where temperature is 1173 K, SiH_2Cl_2 flow rate is 35 sccm, and C_2H_2 flow rate is 180 sccm

Deposition pressure (Pa)	Boat slot	Thickness (μm)	σ_o (MPa)	$E/(1-\nu)$ (GPa)	E (GPa)
267	6	2.70	98	482	401
267	13	2.70	56	484	403
267	20	2.65	27	480	399
				Ave. 482	401

Deposition time is 573 min. (Boat slot 6 is the load end, slot 13 the center, and slot 20 the source end.)

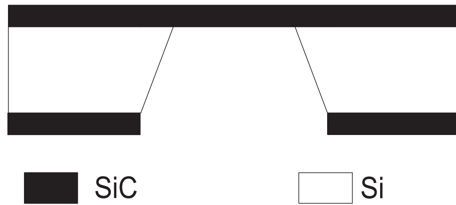

Fig. 2. A cross-sectional schematic of poly-SiC suspended diaphragms fabricated by bulk etching of the (100) silicon substrate from the back side in KOH.

also used to fabricate micro strain gauges. The gauges were fabricated by reactive ion etching using a 2000-Å-thick aluminum etch mask and a CHF_3/O_2 plasma to pattern the poly-SiC films. The free standing sections of the gauges were released by etching the underlying Si substrate in a $HF/HNO_3/CH_3COOH$ solution which does not affect poly-SiC. The sizes of the released structures and the Vernier gauge readings were determined through an optical microscope. Either tensile or compressive strain could be identified immediately after the fabrication and release by inspecting the devices under an optical microscope.

4. Results and discussion

The load-deflection behavior of thin square suspended diaphragms is modeled as [9–11]:

$$P = \frac{t}{a^2} W_o \left[C_1 \sigma_o + \frac{f(v)}{a^2} \frac{E}{1-v} W_o^2 \right] \quad (1)$$

$$P/W_o = \frac{t}{a^2} C_1 \sigma_o + \frac{f(v)t}{a^4} \frac{E}{1-v} W_o^2 \quad (2)$$

where P is an applied pressure, t is the diaphragm (or film) thickness, $2a$ is the length of one edge of the square diaphragm, W_o is the diaphragm center deflection, v is the in-plane Poisson's ratio, σ_o is the film residual stress, $E/(1-v)$ is biaxial modulus, E is Young's modulus, C_1 is a constant equal to 3.41 for square diaphragms [17–22], and $f(v)$ is a dimensionless function of Poisson's ratio which is equal to $1.37(1.446-0.427v)$ [17]. $f(v)$ can be calculated assuming v of 0.168 for polycrystalline 3C-SiC films [29,30]. The residual stress σ_o and biaxial modulus $E/(1-v)$ were calculated by a least-squares fitting of Eq. (1) and a linear fitting of Eq. (2) to experimentally obtain load-deflection data. For "reliable" load-deflection measurements, the corresponding values for σ_o and $E/(1-v)$ obtained from fitting Eqs. (1) and (2) to the data are the same.

For the first set of poly-SiC samples in Section 3 (outlined in Tables 1 and 2), wafers from the center slot position (i.e., slot 13) of a 25-wafer boat were used for the fabrication of diaphragms. The diaphragms fabricated from the poly-SiC films deposited at pressures of 61, 133, and 333 Pa were flat, indicating tensile stress, while those from the films deposited at pressures 380, 500, and 666 Pa were buckled, indicating compressive stress. The flat diaphragms from the three tensile poly-SiC films were used for investigating the effect of the deposition pressure on the residual film stress and in-plane biaxial modulus. Typical load-deflection data along with fits of Eq. (1) for these samples are shown in Fig. 4. Fig. 5 shows the corresponding linear plots of P/W_o to W_o^2 and fits of Eq. (2).

Table 1 presents the average values of residual stress and elastic modulus for the studied poly-SiC films, which were 0.46 to 0.65 μm in thickness. The residual stresses of the films deposited at 61, 133, and 333 Pa were 726, 584, and 265 MPa, respectively. These results are consistent with those measured by the wafer curvature technique and previously reported [8] and confirm that the residual stress of poly-SiC deposited by LPCVD using SiH_2Cl_2 and C_2H_2

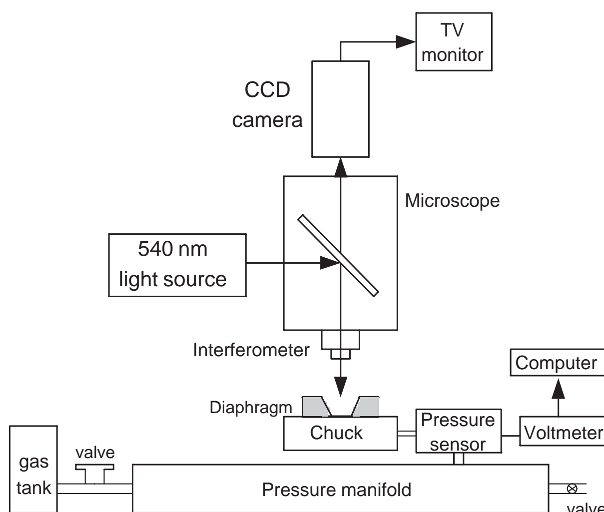

Fig. 3. A schematic diagram of the interferometric load-deflection measurement apparatus.

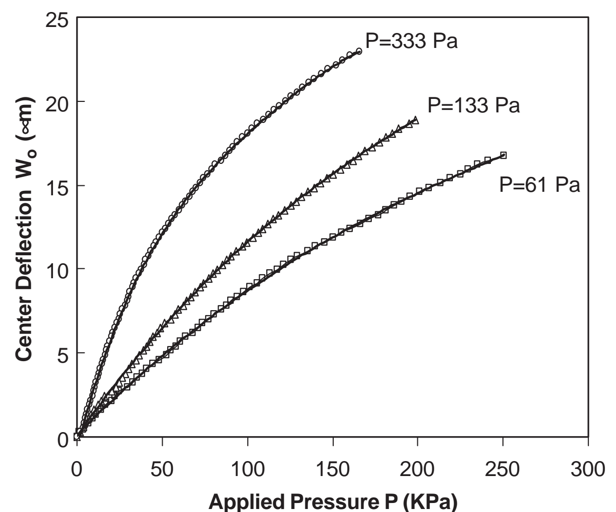

Fig. 4. Load-deflection data from 1×1 mm^2 diaphragms fabricated from poly-SiC films deposited at 61, 133, and 333 Pa at 1173 K with a SiH_2Cl_2 flow rate of 54 sccm and a C_2H_2 flow rate of 180 sccm. The fit of Eq. (1) to the data is also shown.

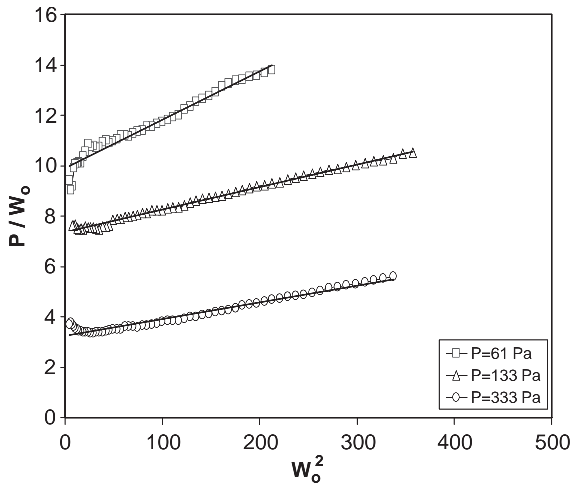

Fig. 5. Linear plots of the load-deflection data of Fig. 4 and the associated fits of Eq. (2).

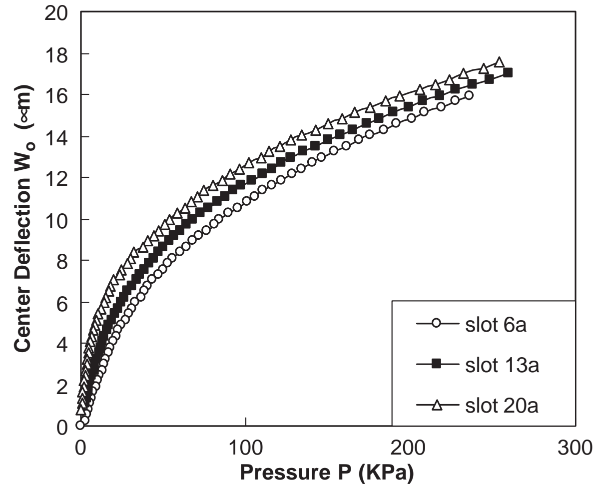

Fig. 6. Load-deflection data from 1×1 mm^2 diaphragms fabricated from poly-SiC films deposited in the same run at 267 Pa, 1173 K, SiH_2Cl_2 flow rate of 35 sccm, and C_2H_2 flow rates of 180 sccm on wafers in boat slots 6 (load end), 13 (center), and 20 (source end).

dual precursors depends on the deposition pressure [8]. The repeatability of residual stress was good for all tested samples, but the modulus measurements from the samples deposited at 61 Pa were poor (i.e., standard deviation higher than 10%) due to their high tensile residual stress. The poor linear fit of Eq. (2) to the load-deflection data for the samples deposited at 61 Pa (0.46 Torr), having high residual tensile stress, can be seen in Fig. 5. High residual film stress added larger deviation to the extracted values for biaxial modulus because the membrane deflections were large enough for the related stress component to be significant in the load-deflection behavior. The slopes of the lines in Fig. 5 indicate the biaxial modulus. The parallel lines associated with the samples deposited at 133 Pa and 333 Pa indicate similar biaxial modulus, given that the membrane size and thickness of the films are the same, as can be seen from Eq. (2). It was also observed that for the high residual tensile stress films deposited at 61 Pa, there was deflection fluctuation (the interference rings would disappear and reappear) as the applied pressure decreased, the cause of which could not be identified. The average biaxial modulus of the three poly-SiC films deposited at 61, 133, and 333 Pa was 476 GPa; accordingly, the average Young's modulus was 396 GPa, assuming v of 0.168 for polycrystalline 3C-SiC films [29,30].

From the second set of samples in Section 3 (outlined in Table 3), low tensile stress, thicker poly-SiC films (i.e., 2.65 to 2.70 μm) were obtained to accurately determine elastic modulus. These depositions at 267 Pa were also used to characterize the residual stress variations as a function of wafer position in the boat. Films deposited on wafers located in slots 6 (load end), 13 (center), and 20 (source end) of a 25-wafer boat were used for diaphragm fabrication. Fig. 6 shows typical load-deflection data along with Eq. (1) fits for three typical samples from the three wafers along the boat. Fig. 7 shows the corresponding linearized fits of Eq. (2) to the load-deflection data in Fig. 6. The good linear relationship between P/W_o and W_o^2 indicates that the measurements were reliable. Fig. 7 shows that the three samples have very similar slopes, which indicates that the in-plane biaxial modulus for the samples is essentially the same, which in turn indicates that the preferred crystalline orientation is the same (i.e., highly textured (111)) [8]. Table 3 lists the calculated average values of σ_o and biaxial modulus $E/(1-v)$. The average biaxial modulus for each film is very close among the three wafer positions, and the average biaxial modulus for the films from all three wafer positions is 482 GPa. Accordingly, the average Young's modulus is 401 GPa, assuming v of 0.168 for polycrystalline 3C-SiC films [29,30]. The residual stress varies substantially even though the film thickness uniformity along the boat is within 4%. The average residual stress is 98 MPa for slot 6, 56 MPa for slot 13, and 27 MPa for 20.

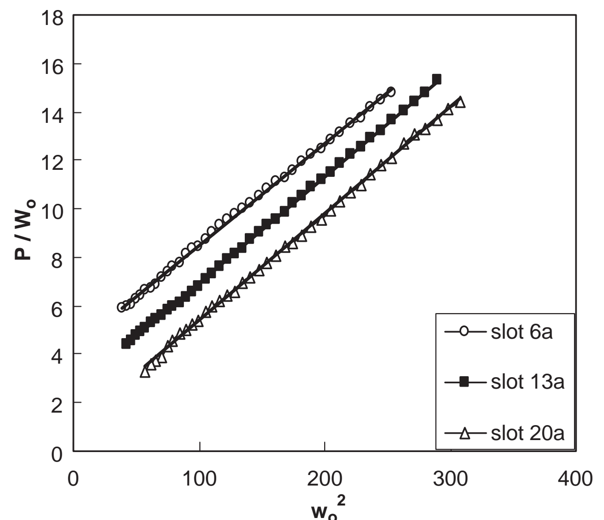

Fig. 7. Linear plots of the load-deflection data of Fig. 6 and the associated fits of Eq. (2).

Clearly, wafer position along the 25-wafer boat significantly affects the residual stress even in the face of very good deposition rate and elastic modulus uniformity. The cause of the variation in residual stress along the boat is not clear. It is suspected that the microstructure differences such as stacking faults, dislocations, and columnar structure are possible factors contributing to the residual stress dissimilarities among the various positions in the wafer boat.

Interestingly, the tensile residual stresses of the films deposited at a pressure of 333 Pa and SiH_2Cl_2 flow rate of 54 sccm are higher than those of the films deposited at a pressure of 267 Pa and SiH_2Cl_2 flow rate of 35 sccm. The former were part of the first set of samples (Tables 1 and 2), which were deposited while the reactor was configured with two precursor injection tubes underneath the wafer boat, and the latter part of the second set of samples (Table 3) without the injection tubes. Based on the findings of the first set of samples and our previous work [8], the higher tensile stress in the former is opposite what would be expected and is attributed to the difference in the precursor injection scheme described in Section 3. The difference in the precursor injection scheme would also explain the against-expected-trend difference in the deposition rate from the former to the latter (i.e., higher pressure and more SiH_2Cl_2 should lead to increased deposition rate). The residual stress of poly-SiC decreases in the tensile range and changes to compressive as SiH_2Cl_2 flow rate was increased, while at fixed deposition pressure of 267 Pa and temperature of 1173 K [31], which excludes the SiH_2Cl_2 flow rate difference in these runs as the cause.

Poly-SiC films deposited at pressures of 61 to 666 Pa were all (111) oriented polycrystalline 3C-SiC and transmission electron microscopy (TEM) indicated that both the tensile and compressive films were columnar in microstructure, with slight differences in the axial alignment of the grains with respect to the film/substrate interface [8].

3C-SiC films with tensile and compressive stresses grown by APCVD have been reported [32,33], for which residual stress has been attributed to the early stage of SiC film growth. Poly-SiC films with tensile and compressive stresses deposited by LPCVD under different temperatures have also been reported [34,35]. SiC films deposited below 1373 K have a columnar structure, are highly oriented along (111), and show compressive stress. Those deposited at 1403 K are randomly oriented, with an equiaxial grain shape, and have tensile residual stress. These results indicate that microstructure is the main determinant of the residual stress of SiC films grown by chemical vapor deposition [35–39]. The current Young's modulus, ~401 GPa, is higher than that (350 GPa) of poly-SiC deposited by APCVD at 1553 K on as-deposited conventional LPCVD poly-Si, but lower than that (460 GPa) of the same poly-SiC deposited on conventional LPCVD poly-Si annealed at 1553 K prior to poly-SiC deposition [23]. The former poly-SiC consists of (110) oriented crystalline and fine columnar grains through the film which are very similar to the grain microstructure of as-deposited poly-Si, while the latter poly-SiC consists of (111) and (110) oriented crystalline grains which are randomly oriented, equiaxed, and non-columnar [23]. Comparing these results leads to the conclusion that (111) crystalline orientation and randomly oriented equiaxed grains result in higher elastic modulus.

Micro strain gauges were fabricated to measure tensile and compressive residual strains of the films deposited at 333, 500, and 666 Pa. Even though the films deposited at 380 Pa were seen to be compressive because of buckled diaphragms, they were not included in the strain gauge study due to time constraints. Details of the mechanics and design points for micro strain gauges have been described previously [28]. Fig. 8(a) shows a scanning electron

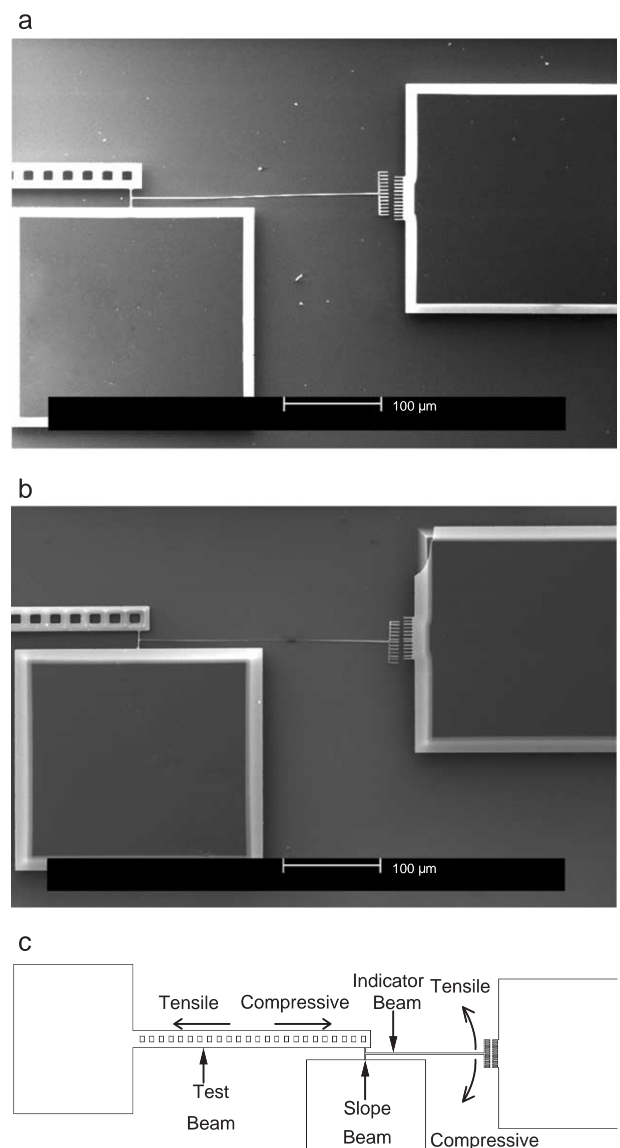

Fig. 8. (a) SEM micrograph of a micro strain gauge fabricated from a 0.52-μm-thick tensile stress poly-SiC film deposited at 333 Pa; (b) SEM micrograph of a micro strain gauge fabricated from a 0.49-μm-thick compressive stress poly-SiC film deposited at 500 Pa; and (c) schematic illustration of a micro strain gauge with tensile or compressive stress.

microscope (SEM) micrograph of a micro strain gauge from a tensile poly-SiC film and Fig. 8(b) shows a SEM micrograph from a compressive poly-SiC film. The strains were calculated based on the readings of a Vernier gauge and the geometry of the micro strain gauges using the equation shown below [28]:

$$\varepsilon = \frac{2L_{sb}\delta_v}{3L_{ib}L_{tb}C} \quad (3)$$

$$C = \frac{1-d^2}{1-d^3} \quad (4)$$

where ε is the strain, and δ is the measured movement at the Vernier gauge site. L_{tb} is the length of the test beam, L_{sb} is the length of the slope beam, and L_{ib} is the length of the indicator beam. C is a correction factor due to the presence of the indicator beam. d is the ratio of the width of the indicator beam w_{ib} over the length of the slope beam L_{sb}. For the strain gauge shown in Fig. 8, the value of C is 0.991. The average Young's modulus of 401 GPa obtained from the second set of films described above was used for the calculation of residual stress. From devices such as that in Fig. 8(a), a value of 0.041% tensile strain is observed and a tensile residual stress of 165 MPa is calculated for the films deposited at 333 Pa. From devices such as that in Fig. 8(b), a value of −0.032% (i.e., compressive) strain is observed and a compressive residual stress of −129 MPa is calculated for the films deposited at 500 Pa. Table 2 presents the measured strains and calculated residual stresses for the studied samples. The residual stress values are in good agreement with those measured from wafer curvature technique. Since the poly-SiC films deposited at 333 Pa used for micro strain gauges and diaphragms were from wafers in different boat position, the differing values (i.e., 165 MPa from micro strain gauges and 265 MPa from diaphragms) confirm that residual stresses vary along the boat as discussed above.

The load-deflection measurement results in Table 1 and micro strain gauge results in Table 2 illustrate the effect of deposition pressure on the residual stress of the deposited poly-SiC films. As the deposition pressure increased from 61 to 666 Pa, the residual stress of the films changed from highly tensile to moderately tensile-to-low compressive. The effect of deposition pressure change from 61 to 666 Pa on poly-SiC film crystalline orientation and microstructure has been investigated using XRD and TEM [8]. XRD analysis indicated that all the films were highly textured (111) orientated polycrystalline 3C-SiC regardless of deposition pressure. The average crystalline size as calculated from the XRD data decreased slightly with increasing deposition pressure. TEM micrographs indicated that all films deposited at pressure from 61 to 666 Pa exhibited columnar grain microstructures [8]. The films deposited at 133 Pa have high tensile stress and have microtwins and columnar grains inclined to the growth direction. The films grown at 666 Pa have grains nearly parallel to the growth direction due to the higher growth rate at a higher deposition pressure. The residual film stress has been attributed to the columnar grain size, shape and stacking faults present in these films [8].

5. Conclusions

Poly-SiC thin films were deposited on 100- and 150-mm-diameter silicon wafers in a high-throughput LPCVD reactor at 1173 K using SiH_2Cl_2 and C_2H_2 precursors. As the deposition pressure was changed from 61 to 666 Pa, the films exhibited residual stresses that varied from highly tensile (e.g., 726 MPa) to moderately tensile-to-low compressive (e.g., −98 MPa). The residual stress changed sign in the 333 to 380 Pa deposition pressure range. The residual stresses of the deposited SiC films can therefore be controlled by adjusting the deposition pressure without impacting the process thermal budget.

The residual stresses varied significantly from wafer to wafer along the 25-wafer boat for the same deposition, while the elastic modulus did not change, which indicates that the preferred crystalline orientation and grain structure remained the same. An average Young's modulus of 401 GPa was obtained from reliable load-deflections measurements on low tensile stress thick films (around 2.7 μm). The modulus and stress data reported in this study check favorably against results from measurements using other techniques on similarly deposited films in our previous studies and establish basic mechanical properties data to support MEMS device design based on poly-SiC.

Acknowledgements

This work was funded by DARPA (Contract # DABT63-98-1-0010) and the Glennan Microsystems Initiative. The authors would also like to thank Mr. Ronald Jezeski for his assistance during LPCVD SiC depositions. One or more of the authors have a significant financial interest in the products or methods being investigated in this study.

References

[1] M. Mehregany, C.A. Zorman, S. Roy, A.J. Fleischman, C.H. Wu, N. Rajan, Int. Mater. Rev. 45 (2000) 85.
[2] P.M. Sarro, Sens. Actuators, A, Phys. 82 (2000) 210.
[3] M. Mehregany, C.A. Zorman, Thin Solid Films 355–356 (1999) 518.
[4] M. Mehregany, C.A. Zorman, N. Rajan, C.H. Wu, Proc. IEEE 86 (1998) 594.
[5] D. Gao, B.J. Wijesundara, C. Carraro, R.T. Howe, R. Maboudian, IEEE Sens. J. 4 (2004) 441.
[6] X. Song, S. Rajgopal, J.M. Melzak, C.A. Zorman, M. Mehregany, Mat. Sci. Forum 389–393 (2002) 755.
[7] M.B.J. Wijesundara, G. Valente, W.R. Ashurst, R.T. Howe, A.P. Pisano, C. Carraro, R. Maboudian, J. Electrochem. Soc. 151 (2004) C210.

[8] X.A. Fu, R. Jezeski, C.A. Zorman, M. Mehregany, Appl. Phys. Lett. 84 (2004) 341.
[9] C.A. Zorman, S. Rajgopal, X.A. Fu, R. Jezeski, J. Melzak, M. Mehregany, Electrochem. Solid-State Lett. 5 (2002) G99.
[10] N. Rajan, C.A. Zorman, S. Stefanescu, M. Mehregany, T.P. Kicher, J. Microelectromech. Syst. 8 (1999) 251.
[11] C.H. Wu, S. Stefanescu, H.I. Kuo, C.A. Zorman, M. Mehregany, Technical Digest—11th Int. Conf. on Solid State Sensor and Actuators-Eurosensors XV, Munich, Germany, 2001, p. 514.
[12] K.N. Vinod, C.A. Zorman, M. Mehregany, Technical Digest—1997 Int. Conf. on Solid State Sensors and Actuators, Chicago, I1, 1997, p. 653.
[13] X. Song, S. Guo, C.A. Zorman, C.H. Wu, A. Yasseen, M. Mehregany, Proc. of the Int. Conf. on Silicon Carbide and Related Materials, Research Triangle Park, NC, 1999, p. 1145.
[14] A.A. Yasseen, C.H. Wu, C.A. Zorman, M. Mehregany, IEEE Electron Device Lett. 21 (2000) 164.
[15] D.J. Young, J. Du, C.A. Zorman, W.H. Ko, IEEE Sens. J. 4 (2004) 464.
[16] S. Roy, R.G. DeAnna, C.A. Zorman, M. Mehregany, IEEE Trans. Electron Devices 49 (2002) 2323.
[17] J.Y. Pan, P. Lin, F. Maseeh, S.D. Senturia, Technical Digest, IEEE Solid-State Sensor and Actuator Workshop, Hilton Head, S.C. 191, 1990, p. 70.
[18] D. Maier-Schneider, A. Koprululu, S.B. Holm, E. Obermeier, J. Micromechanics Microengineering 6 (1996) 436.
[19] J.J. Vlassak, W.D. Nix, J. Mater. Res. Soc. 7 (1992) 3242.
[20] L. Tong, M. Mehregany, Appl. Phys. Lett. 60 (1992) 2992.
[21] M. Mehregany, L. Tong, L.G. Matus, D.J. Larkin, IEEE Trans. Electron Devices 44 (1997) 74.
[22] J.S. Mitchell, C.A. Zorman, T. Kicher, S. Roy, M. Mehregany, J. Aerosp. Eng. 16 (2003) 46.
[23] S. Roy, C.A. Zorman, M. Mehregany, Mat. Res. Soc. Symp. Proc., vol. 657, 2001, EE9.5.1-9.5.6.
[24] X.A. Fu, J. Dunning, C.A. Zorman, M. Mehregany, Mat. Sci. Forum 457–460 (2004) 1519.
[25] M. Itoh, M. Hori, H. Komano, I. Mori, J. Vac. Sci. Technol., B 9 (1991) 3262.
[26] K. Murooka, I. Higashikawa, Y. Gomei, Appl. Phys. Lett. 69 (1996) 37.
[27] D. Gao, M.B.J. Wijesundara, C. Carraro, C.W. Low, R.T. Howe, R. Maboudian, Proc. Transducers 12th Int. Conf. Solid-State Sensors and Actuators, 2003, p. 1160.
[28] L.W. Lin, A.P. Pisano, R.T. Howe, J. Microelectromech. Syst. 6 (1997) 313.
[29] W.R.L. Lambrecht, B. Segall, M. Methfessel, W. van Schilfgarrde, Phys. Rev., B 44 (1991) 3685.
[30] R.D. Carnahan, J. Am. Ceram. Soc. 51 (1968) 223.
[31] J. Dunning, X.A. Fu, S. Rajgopal, M. Mehregany, C.A. Zorman, Mat. Sci. Forum 457–460 (2004) 1523.
[32] T. Chassagne, G. Ferro, C. Gourbeyre, M. Le Berre, D. Barbier, Y. Monteil, Mat. Sci. Forum 353–356 (2001) 155.
[33] C. Gourbeyre, T. Chassagne, M. Le Berre, G. Ferro, E. Gautier, Y. Monteil, D. Barbier, Sens. Actuators, A, Phys. 99 (2002) 31.
[34] J. Rodriguez-Viejo, E. Hurtos, R. Kressmann, M.T. Clavaguera-Mora, Mat. Sci. Forum 347–3 (2000) 477.
[35] E. Hurtos, J. Rodriguez-Viejo, J. Appl. Phys. 87 (2000) 1748.
[36] Y.M. Lu, I.C. Leu, Surf. Coat. Technol. 124 (2000) 262.
[37] Y.M. Lu, I.C. Leu, Thin Solid Films 377–378 (2000) 389.
[38] Y.H. Yun, S.C. Choi, J. Ceram. Soc. Jpn. 108 (2000) 1045.
[39] Y.H. Yun, S.C. Choi, J.C. Chang, J.C. Kim, J. Ceram Process. Res. 2 (2001) 129.